

Spin-Density Relaxation in Superfluid $^3\text{He-A}_1$

S. T. Lu, Qiang Jiang, and Haruo Kojima

Serin Physics Laboratory, Rutgers University, Piscataway, New Jersey 08854

(Received 3 August 1988)

We report measurements on the spin-density relaxation in the superfluid $^3\text{He-A}_1$ phase as a function of temperature, pressure (3–28 bars), and magnetic field (0.75–14 kOe). The temperature dependence of the relaxation time shows an unexpected discontinuity near the middle of the phase and very close to T_c (the zero-field transition temperature). The relaxation time changes only by about 30% over the pressure range measured. In the higher-temperature side of the phase the relaxation time is proportional to the applied field.

PACS numbers: 67.50.Fi

In the superfluid phases of Fermi liquid ^3He , both mass and spin supercurrents can be induced.¹ In the A and B phases, the two types of supercurrents can exist independently. The mass superfluidity leads to phenomena such as persistent currents and fourth sound propagation. The spin superfluidity effects have been probed mainly by NMR. Early NMR experiments^{2–5} uncovered puzzling magnetization relaxation effects in both A and B phases. Recently, both experimental^{6,7} and theoretical⁸ work were carried out to show that the puzzling effects arose from the spin supercurrents leading to instability in spin precession in A phase and to formation of magnetization domains in B phase. In the A_1 phase, the two supercurrents are no longer independent of each other. A mass supercurrent is simultaneously a spin supercurrent.⁹ This implies that the spin current effects such as the spin-temperature wave propagation may be measured¹⁰ by a mechanical detector. The A_1 phase spin dynamics has not been measured extensively owing to the technical difficulty in creating the phase in substantial temperature widths in large magnetic fields. We report on new spin-relaxation phenomenon in the A_1 phase measured by a novel mechanical method.

Consider a small chamber (a differential pressure sensor) whose one wall is a flexible diaphragm and another is a stack of parallel superleak channels which connect the interior of the chamber to a large liquid reservoir. The chamber is immersed in A_1 phase liquid produced by a static magnetic field applied along the channels (\hat{z} direction). A gradient in magnetic field can be applied to produce superflow along the same direction. The superfluid component velocity v_s in the superleak is described by an equation of motion given by⁹

$$\partial v_s / \partial t = -(8\pi\sigma/\rho BL)z - (\hbar/2mL)\delta\omega, \quad (1)$$

where z , σ , and B are the displacement, the tension, and the area of the diaphragm, respectively, ρ is the total liquid mass density, L is the length of the superleak, and m the mass of ^3He atom. The difference in angular velocity across the superleak is given by $\delta\omega = \gamma(\gamma\delta S/\chi - \delta H)$, where γ is the absolute value of gyromagnetic

ratio, χ is the magnetic susceptibility, δS is the spin-density difference, and δH is the magnetic field difference across the superleak. The first term of the right-hand side of Eq. (1) is the hydrodynamic pressure gradient across the superleak.¹¹ The thermal drive is small and neglected. We neglect here any effects of magnetic field transverse to the superfluid flow direction. Spatial variations of the orbital anisotropy vector and the spin quantization vector both couple to the superfluid velocity only in second-order derivatives⁹ and these coupling terms are neglected in Eq. (1). In the limit that the fluid is regarded incompressible, the velocity of the diaphragm is related to the fluid velocity by $\dot{z} = (A/B)[(\rho_s/\rho) \times v_s + (\rho_n/\rho)v_n]$, where A is the cross-sectional area of superleak, ρ_s is the superfluid component density, ρ_n is the normal component density, and v_n is the normal component velocity. In the dc flow limit, the normal component velocity is given by $v_n = -(8\pi\sigma/\rho BLR)z$, where R is the flow resistance of the channels. The measurement of z as a function of time then allows us to determine the time dependence of $\delta\omega$, and hence δS , in response to a known externally applied field gradient.

To reduce construction time, we removed and used the differential pressure sensor intact from our previous setup.¹² The superleak made of Stycast 1266 epoxy was a stack of ten parallel channels of height = 25 μm , width = 6.5 mm, and length (along \hat{z}) = 3.3 mm. The large normal fluid flow resistance of the channels (e.g., $R = 3.5 \times 10^6 \text{ sec}^{-1}$ at 2.6 mK and 24 bars) allowed us to neglect the normal component acceleration. The tension σ of the diaphragm was $2.2 \times 10^5 \text{ dyn/cm}$. The change δc in capacitance between the diaphragm and the fixed plate was measured by an ac bridge operating at 1 kHz. The diaphragm displacement is related to δc by $z = (\delta c/c_0)z_0$, where c_0 and z_0 are the ambient capacitance and the separation of the capacitor plates, respectively. The sensor was immersed in liquid ^3He (with less than 10 ppm He^4) and placed into our new PrNi₅ nuclear demagnetization apparatus.¹³ A new superconducting magnet¹⁴ capable of applying static fields up to 17 kOe in the sensor region for creating the A_1 phase was made and in-

incorporated into the demagnetization apparatus. The magnetic field was measured to be homogeneous to 0.2% within 1.0 cm of the center of the magnet. Another set of coils was placed inside the magnet for applying a linear field gradient along the superleak. The static and the gradient field coils were both anchored to the mixing chamber of a dilution refrigerator. The temperature was derived from the magnetic susceptibility of La-diluted cerium-magnesium-nitrate powder immersed in the liquid ^3He and calibrated against the ^3He phase diaphragm of Greywall.¹⁵ The temperature width of the A_1 phase as measured by magnetically driven superflow was reproducible within 2% and in agreement depending on pressure within 2%–15% of the phase diagram measurement by Israelsson *et al.*¹⁶ and 2%–17% of that by Sagan *et al.*¹⁷

Examples of the measured diaphragm displacement z as a function of time and the magnetization difference

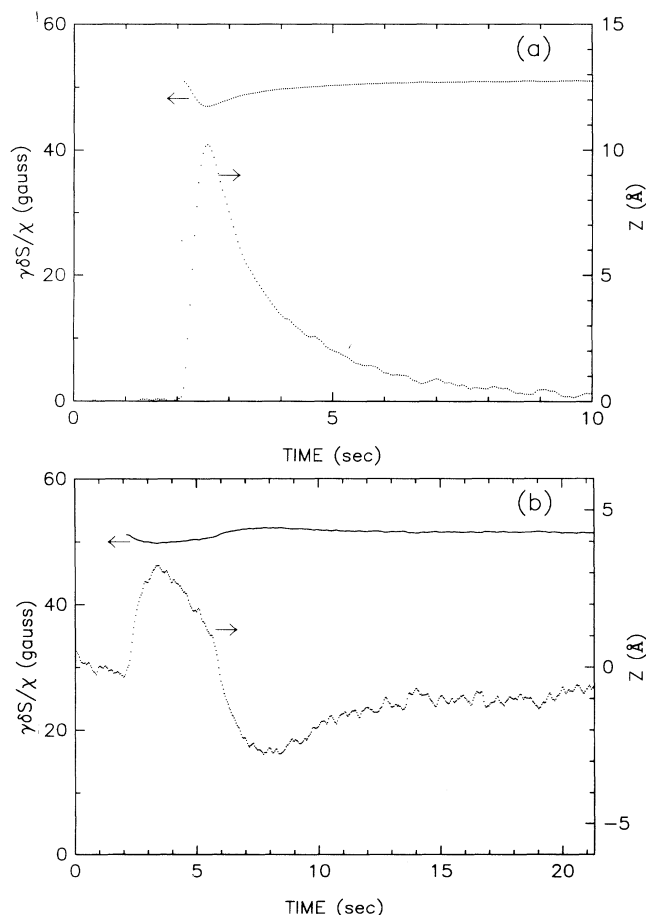


FIG. 1. Examples of measured diaphragm response (z) and derived magnetization difference across the superleak ($\gamma\delta S/\chi$). The pressure was 7.0 bars. The applied static magnetic field was 9.2 kOe. The sampling time interval was 41.6 msec. The normalized reduced temperature was $r=0.40$ and 0.03 and averaged 25 and 5 times for (a) and (b), respectively.

$\gamma\delta S/\chi$ derived from it are shown in Fig. 1. The field gradient was kept constant at -77 G/cm for $t < 2$ sec, increased linearly to $+77$ G/cm within a ramp time of 100 msec, and then kept constant for observing the relaxation. The computation of δS was simple since $z(t)$ dominated over its time-derivative terms by 2 orders of magnitude. As the field gradient ramps up and the superfluid component (carrying fully polarized spin) flows into the small chamber at essentially constant velocity, the displacement and the spin-density gradient increase linearly. After the field gradient becomes constant, z continues to increase transiently before it finally begins to relax towards zero. The transient increase in z shows up as a dip in the spin-density gradient before it relaxes towards the final equilibrium value $\chi\delta H/\gamma$. The conversion of the superfluid spin into quasiparticle spin is thought to occur on a short-time scale of quasiparticle relaxation time ($\sim \mu\text{sec}$). The transient behavior may result from the time required for spatial dispersion of spins initially localized near the edges of the superleak channels. Over most of the temperature range (II and III of Fig. 2), the final relaxation was exponential as shown in Fig. 1(a). In this case, the relaxation time τ was determined by a least-squares fit to exponential decay. The relaxation time showed no systematic dependence on the ramp time and the relaxation time was constant within the scatter of 10% for ramp rates between 11×10^3 and 1.7×10^3 G/cm sec. The relaxation time did not depend on the magnitude of the final field gradient left on in the range from -77 to 77 G/cm. Very close to T_{c1} , the spin-density recovery was nonexponential as shown in Fig. 1(b). The spin density overshoot before finally relaxing to its equilibrium value.

The temperature dependence of the relaxation time as a function of the normalized reduced temperature, $r = (T_{c1} - T)/(T_{c1} - T_{c2})$, is shown in Fig. 2. T_{c1} and T_{c2} are the A_1 - N and A_2 - A_1 transition temperatures, respec-

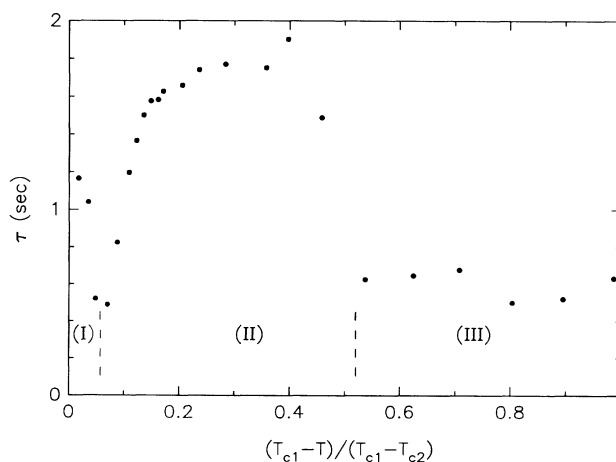


FIG. 2. Relaxation time and "time constant" (see text) as functions of normalized reduced temperature at $p = 7.0$ bars.

tively. The liquid pressure was 7.0 bars and the applied static magnetic field was 9.2 kOe. The temperature dependence can be divided into three regions. In regions II and III the relaxation was exponential and they were separated by the sharp change of relaxation time near $r=0.52$. In region III the relaxation time is relatively short and independent of temperature within the scatter of 10%. The sharp increase at the region II-III boundary occurs within a temperature width less than $2\ \mu\text{K}$. We believe that the apparent rounding is caused by averaging and that there is a discontinuity of τ here. Comparison between the phase diagram¹⁶ and measured pressure dependence of r at the discontinuity showed that the discontinuity occurs at the zero-field transition temperature T_c within 5%.¹⁸ The relaxation time goes through a character minimum. In region I, the relaxation is nonexponential as shown in Fig. 1(b). The region I-II crossover occurs over a narrow temperature range ($\leq 1\ \mu\text{K}$) near the minimum in relaxation time. For the purpose of displaying temperature dependence in the nonexponential region, the "time constant" defined by the time interval that the difference of spin density from its equilibrium value takes to reduce from 90% to 40% of maximum after the decay begins to take place, is plotted in Fig. 2. The time constant increases steeply as T_{c1} is approached.

The measured pressure dependence of the relaxation time at $r=0.40$ (in region II) and 0.90 (in region III) is shown in Fig. 3. The applied static magnetic field was 9.2 kOe. The qualitative temperature dependence was similar to Fig. 2 at all pressures between 5 and 28 bars. The estimated values of the shear viscosity, the second viscosity, and the spin-diffusion coefficient¹⁹ at or near T_c increases by factors of 5.8, 13, and 18, respectively, in decreasing the pressure from 28 to 3 bars. Figure 3 clearly shows that the pressure dependence of τ is much

smaller than this in regions II and III. Neither the normal fluid flow nor spin diffusion alone plays a dominant role in the relaxation phenomenon. We cannot rule out, however, the possibility that the two effects combine to show a relatively small pressure dependence.

The dependence of the relaxation time on the static magnetic field was measured at 23 bars and is shown in Fig. 4 for selected values of normalized reduced temperature. At each field studied, the temperature dependence was measured in the same manner as that of Fig. 2. The general temperature dependence as described by the three regions as in Fig. 2 could be clearly distinguished down to the field of 5 kOe. At fields less than 5 kOe the relative width of region I increased and that of region II decreased. The data in Fig. 4 for which $H \leq 3$ kOe and $r \leq 0.15$ refer to the time constant of region I. In region III (see $r=0.90$ data), τ has little or no dependence on the applied field except in the range $H < 5$ kOe where it may be proportional to the field. In contrast, τ is approximately proportional to H in region II (see $r=0.13, 0.30$, and 0.50 data) in the range $5 < H < 14$ kOe. The proportionality constant decreases as the value of r decreases. The field dependence in region I is difficult to establish because of the sharp temperature dependence as described above.

In the only other experiment on spin-relaxation phenomena in the A_1 phase, Corruccini and Osheroff² measured the longitudinal relaxation time T_1 of the A_1 phase at melting pressure and an applied field of 3.05 kOe using NMR. Within precision there seems to be no anomaly at T_c in their experiment. Since the measured spin-relaxation time is greatly affected by the interface between bounding solid wall and liquid ^3He ,²⁰ it is difficult to draw a firm conclusion from comparison of the two experiments. The observed linear field dependence of the relaxation time above T_c is the same as the field depen-

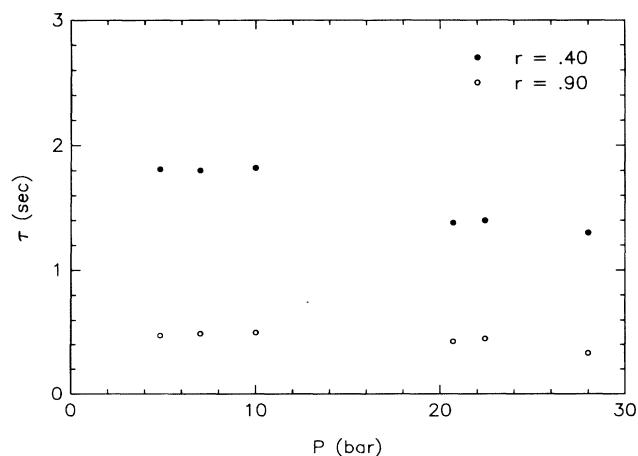


FIG. 3. Pressure dependence of relaxation time for selected values of normalized reduced temperature. The polycritical point pressure is 21 bars.

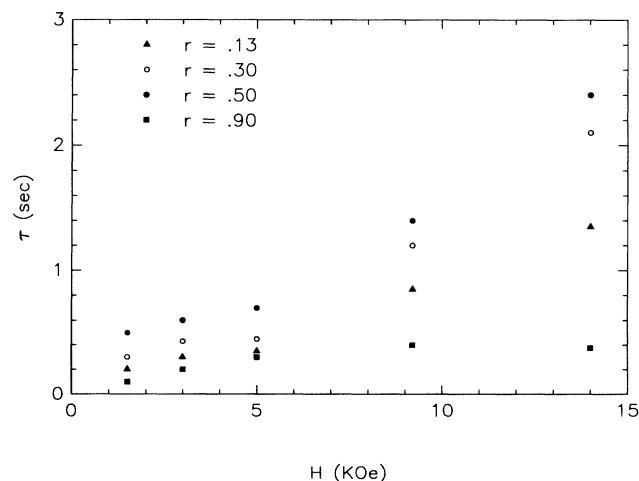


FIG. 4. Static magnetic field dependence of relaxation time at selected values of normalized reduced temperature.

dence of T_1 of liquid ^3He immersed in confined geometries.²⁰ This suggests that the interface boundary layer is important in the spin relaxation in our experiment. If the relaxation is boundary dominated, there remains the puzzle of what mechanism is responsible for apparently turning it off below T_c . Existence of surface superfluid phases²¹ different from that of bulk might lead to the changes in relaxation rates we observe. It would be very interesting to observe how the surface phase (assuming it exists) would be modified by coating the surfaces with a one or two monolayers of nonmagnetic ^4He . Recently it was demonstrated by Freeman *et al.*²² that such a coating on a Mylar substrate could modify the local order-parameter magnitude.

In summary, we have discovered an unexpected discontinuity in the spin-mass flow relaxation in the superfluid ^3He - A_1 phase. The discontinuity occurs near the middle of the phase very close to the zero-field transition temperature. The measured pressure and applied static magnetic field dependence show that the relaxation phenomenon does not result from the usual bulk transport effects such as viscosity, spin diffusion, and thermal conductivity. It is hoped that our experiments will stimulate new theoretical and experimental studies on the magnetohydrodynamic phenomena of the ^3He - A_1 phase.

It is our pleasure to acknowledge advice on the PrNi₅ demagnetization apparatus from Doug Osheroff, Rene Reul, and Dennis Greywall. We thank Val Myrniij and his staff for the expert machining of the apparatus. We thank Paul Busch for providing us with software for a superconducting magnet design. This research was supported in part by National Science Foundation, Low Temperature Physics Program, Grant No. DMR-85-21559.

¹A. J. Leggett, *Rev. Mod. Phys.* **47**, 331 (1975).

²L. R. Corruccini and D. D. Osheroff, *Phys. Rev. B* **17**, 126 (1978).

³R. A. Webb, *Phys. Rev. Lett.* **40**, 883 (1978).

⁴R. E. Sager, R. L. Kleinberg, P. A. Warkentin, and J. C. Wheatley, *J. Low Temp. Phys.* **32**, 263 (1978).

⁵R. W. Giannetta, E. N. Smith, and D. M. Lee, *J. Low*

Temp. Phys. **45**, 295 (1981).

⁶Yu. M. Bunkov, V. V. Dmitriev, and Yu. M. Mukharskii, *Zh. Eksp. Teor. Fiz.* **88**, 1218 (1985) [*Sov. Phys. JETP* **61**, 719 (1985)].

⁷A. S. Borovik-Romanov, Yu. M. Bunkov, V. V. Dmitriev, Yu. M. Mukharskii, and K. Flachbart, *Zh. Eksp. Teor. Fiz.* **88**, 2025 (1985) [*Sov. Phys. JETP* **61**, 1199 (1985)].

⁸I. A. Fomin, *Zh. Eksp. Teor. Fiz.* **88**, 2039 (1985) [*Sov. Phys. JETP* **61**, 1199 (1985)].

⁹M. Liu, *Phys. Rev. Lett.* **43**, 1740 (1979).

¹⁰L. R. Corruccini and D. D. Osheroff, *Phys. Rev. Lett.* **45**, 2029 (1980).

¹¹The flow impedance of the space surrounding the sensor and connecting the back of the diaphragm and the reservoir side of the superleak channels is estimated to be smaller than that of the superleak by a factor of 133. Thus, to a good accuracy, the pressure difference across the diaphragm is equal to the pressure difference across the superleak.

¹²R. Ruel and H. Kojima, *Phys. Rev. Lett.* **54**, 2238 (1985).

¹³S. T. Lu, Q. Jiang, and H. Kojima, *Bull. Am. Phys. Soc.* **33**, 407 (1988).

¹⁴Our magnet contained active and passive shielding designs similar to those of U. E. Israelsson and C. M. Gould, *Rev. Sci. Instrum.* **55**, 1143 (1984).

¹⁵D. Greywall, *Phys. Rev. B* **33**, 7520 (1986).

¹⁶U. E. Israelsson, B. C. Crooker, H. M. Bozler, and C. M. Gould, *Phys. Rev. Lett.* **53**, 1943 (1984).

¹⁷D. C. Sagan *et al.*, *Phys. Rev. Lett.* **53**, 1939 (1984).

¹⁸The conclusion that the discontinuity in τ occurs in the A_1 phase and not in other low-field regions is supported by (1) the fringing field of the static field becomes zero at more than 3.6 cm away from the superleak, (2) the driving magnetic field gradient in the zero-field region is lower than the A_1 phase region by a factor of 10^{-3} , and (3) two other "discontinuities" (marked by disappearance of signal) are observed at T_{c1} and T_{c2} ($< T_c$) and no transition is expected in zero-field phase below T_c .

¹⁹J. C. Wheatley, in *Quantum Fluids*, edited by D. F. Brewer (North-Holland, Amsterdam, 1966).

²⁰R. C. Richardson, *Physica* (Amsterdam) **126B**, 298 (1984).

²¹For a recent study on surface phase diagram, see Y. H. Li and T. L. Ho, *Phys. Rev. B* **38**, 2362 (1988).

²²M. R. Freeman, R. S. Germain, E. V. Thuneberg, and R. C. Richardson, *Phys. Rev. Lett.* **60**, 596 (1988). The "tuning" of the order parameter occurs over a distance of the order of coherence length (a few hundred Å). For the ^4He coating to affect our experiment (with superleak dimension of 25 μm) the relevant distance scale would have to be much greater.